Published in final edited form as:

J Neurosci Res. 2020 October ; 98(10): 2096–2108. doi:10.1002/jnr.24684.

Degron capability of the hydrophobic C-terminus of the polyglutamine disease protein, ataxin-3

Jessica R. Blount[1], **Sean L. Johnson**[1], **Kozeta Libohova**[1], **Sokol V. Todi**[1,2], **Wei-Ling Tsou**[1]

[1]Department of Pharmacology, Wayne State University School of Medicine, Detroit, MI, USA

[2]Department of Neurology, Wayne State University School of Medicine, Detroit, MI, USA

Abstract

Ataxin-3 is a deubiquitinase and polyglutamine disease protein whose cellular properties and functions are not entirely understood. Mutations in ataxin-3 cause spinocerebellar ataxia type 3 (SCA3), a neurodegenerative disorder that is a member of the polyglutamine family of diseases. Two major isoforms arise from alternative splicing of *ATXN3* and are differently toxic *in vivo* as a result of faster proteasomal degradation of one isoform compared to the other. The isoforms vary only at their C-termini, suggesting that the hydrophobic C-terminus of the more quickly degraded form of ataxin-3 (here referred to as isoform 2) functions as a degron–that is, a peptide sequence that expedites the degradation of its host protein. We explored this notion in this study and present evidence that: (a) the C-terminus of ataxin-3 isoform 2 signals its degradation in a proteasome-dependent manner, (b) this effect from the C-terminus of isoform 2 does not require the ubiquitination of ataxin-3, and (c) the isolated C-terminus of isoform 2 can enhance the degradation of an unrelated protein. According to our data, the C-terminus of ataxin-3 isoform 2 is a degron, increasing overall understanding of the cellular properties of the SCA3 protein.

Keywords

ataxia; deubiquitinase; isoform; neurodegeneration; polyglutamine; proteasome; RRID:AB_1281300; RRID:AB_2307391; RRID:SCR_001010; ubiquitin

Correspondence: Wei-Ling Tsou, Department of Pharmacology, Wayne State University School of Medicine, 540 E. Canfield, Scott Hall, Detroit, MI 48201, USA. wtsou@wayne.edu.

AUTHOR CONTRIBUTIONS

Conceptualization: JRB, SVT, W-LT; *Investigation*: JRB, SLJ, KL, SVT, W-LT; *Formal analysis*: JRB, SLJ, SVT, W-LT; *Visualization*: JRB, SVT, W-LT; *Writing*: JRB, SVT, W-LT; *Funding acquisition*: JRB, SLJ, SVT.

CONFLICT OF INTEREST

The authors declare no conflict of interest.

Declaration of Transparency

The authors, reviewers and editors affirm that in accordance to the policies set by the *Journal of Neuroscience Research*, this manuscript presents an accurate and transparent account of the study being reported and that all critical details describing the methods and results are present.

SUPPORTING INFORMATION

Additional supporting information may be found online in the Supporting Information section.

Transparent Peer Review Report

Transparent Science Questionnaire for Authors

1 | INTRODUCTION

Degradation of most proteins in eukaryotic cells is conducted by the ubiquitin-proteasome system (Budenholzer, Cheng, Li, & Hochstrasser, 2017; Chau et al., 1989; Collins & Goldberg, 2017; Heride, Urbe, & Clague, 2014; Thibaudeau & Smith, 2019; Thrower, Hoffman, Rechsteiner, & Pickart, 2000). A protein designated for degradation is marked by a ubiquitin signal–commonly a poly-ubiquitin chain–that is recognized by the proteasome, where ubiquitin is removed to be recycled and the target protein is degraded (Budenholzer et al., 2017; Collins & Goldberg, 2017; Kraut, Prakash, & Matouschek, 2007; Thibaudeau & Smith, 2019). How that degradation-destined protein is specifically recognized and ubiquitinated by the appropriate machinery is a long-studied question whose answers are varied, complex, and still not entirely known (Ciechanover & Stanhill, 2014; Finley, 2009; Grice & Nathan, 2016; Saeki, 2017). Substrate recognition and ubiquitination can depend on many factors, including the substrate's amino acid sequence, its folding, and any post-translational modifications it already has (Ciechanover & Stanhill, 2014; Collins & Goldberg, 2017; Lucas & Ciulli, 2017; Schreiber & Peter, 2014). These substrate-specific properties that signal proteasomal degradation are termed degrons.

Degrons can be either inherent or acquired (Ella, Reiss, & Ravid, 2019); those that arise directly from amino acid sequences are deemed inherent, while acquired degrons are a consequence of post-translational modifications that can promote ubiquitination, like phosphorylation or SUMOylation. In many cases, inherent degrons are hydrophobic amino acid sequences that are increasingly exposed when their host protein is folded improperly, leading to its ubiquitination as part of the protein quality control process (Amm, Sommer, & Wolf, 2014; Ella et al., 2019; Erales & Coffino, 2014; Varshavsky, 2017, 2019). Many degrons that have already been characterized include internal lysine residues, where poly-ubiquitin chains can be attached for proteasomal targeting (Varshavsky, 2019), while there are some ubiquitin-independent degrons that do not require the attachment of poly-ubiquitin for their host proteins' degradation (Erales & Coffino, 2014; Sanchez-Lanzas & Castano, 2014). To trigger the removal of a protein, ubiquitin-independent degrons may rely on protein folding, the hydrophobicity of amino acid residues, or binding partners (Erales & Coffino, 2014). Specific and timely removal of proteins–both normally and abnormally folded ones–through the proteasome system is critical for maintaining cellular homeostasis and health in the whole organism (Jariel-Encontre, Bossis, & Piechaczyk, 2008). Identifying and classifying different types of degrons is therefore critical for understanding the protein degradation process (Ella et al., 2019; Erales & Coffino, 2014; Varshavsky, 2019).

Our interest in degron-based protein degradation arose from recent work with the deubiquitinase and polyglutamine (polyQ) disease protein, ataxin-3 (Blount et al., 2014; Johnson et al., 2019; Ristic, Sutton, Libohova, & Todi, 2018; Ristic, Tsou, & Todi, 2014; Sutton et al., 2017). Ataxin-3 contains a polyQ stretch in its C-terminal half that, when abnormally expanded, causes neurodegeneration in the age-related disease, spinocerebellar ataxia type 3 (SCA3), also known as Machado-Joseph Disease (Costa Mdo & Paulson, 2012; Matos, de Almeida, & Nobrega, 2019; Paulson, 2007). The *ATXN3* gene leads to the production of different isoforms of ataxin-3 (Figure 1; Harris, Dodelzon, Gong, Gonzalez-Alegre, & Paulson, 2010; Johnson et al., 2019; Schmidt et al., 1998; Schmidt et

al., 2019). These isoforms contain the same N-terminal deubiquitinase (Josephin) domain, ubiquitin-interacting motifs (UIMs) 1 and 2, and polyQ stretch, but differ at their C-termini. One isoform (denoted here as isoform 1) contains a third UIM, whereas the other contains a hydrophobic tail (isoform 2). Isoform 2 also exists as a single-nucleotide polymorphism (SNP) variant that terminates earlier (isoform 2 truncated; Figure 1). Isoform 1 is the predominant species in mammalian brain, although isoform 2 is also present (Harris et al., 2010; Schmidt et al., 1998).

We recently examined the toxic proprieties of isoforms 1 and 2 of ataxin-3 *in vivo*, using the model organism *Drosophila melanogaster* (Johnson et al., 2019). We found that isoform 1 is markedly and consistently more toxic than isoform 2. The two isoforms differ in their protein levels and turnover properties, with isoform 2 being degraded significantly more rapidly in flies and in mammalian cells. Additional studies showed that fusing the hydrophobic tail of isoform 2 of ataxin-3 onto the more stable isoform 1 renders the resulting protein dramatically less stable (Johnson et al., 2019). This last datum presented the possibility that the C-terminal hydrophobic residues of ataxin-3 isoform 2 function as a degron. Here, we present results that the C-terminus of isoform 2 is a degron, without the need of ataxin-3 to be ubiquitinated to be degraded. Our findings provide new information on the handling of ataxin-3 in the cell and open the possibility that sequences similar in folding to its hydrophobic tail function as degrons in other proteins.

2 | MATERIALS AND METHODS

The various reagents and tools used are summarized in Table 1.

2.1 | Antibodies

Anti-ataxin-3 (MJD; rabbit polyclonal, 1:15,000; Paulson et al., 1997), anti-GFP (rabbit monoclonal, 1:1,000; Cell Signaling), peroxidase-conjugated secondary antibody (goat anti-rabbit, 1:10,000; Jackson Immunoresearch).

2.2 | Plasmids, mammalian cells, and transfections

Ataxin-3 and eGFP variants were synthesized by the company Genscript (genscript.com) and subcloned into HA-tagged, pCDNA3.1(+1) for ataxin-3 or pCDNA3.1+N-eGFP for eGFP. The identity and integrity of all plasmids used in this work were confirmed through site-restricted digests as well as two rounds of sequencing by the vendor and by our group. HEK-293T cells were purchased from ATCC, confirmed for lack of mycoplasma contamination, and cultured in DMEM supplemented with 10% FBS and 5% penicillin-streptomycin, under conventional conditions at 37°C and 5% CO_2. The day before transfection, cells were trypsinized, resuspended, and seeded on 12-well or 24-well plates. Cells were then transfected with the plasmids indicated in figures using Lipofectamine LTX (Thermo Fisher) following the manufacturer's protocols. The same total amount of plasmid was transfected into each well for each experimental group, helping to ensure consistent transfection efficiency. Twenty-four hours after transfection, cells were treated with MG132, chloroquine, or cycloheximide (each purchased from A. G. Scientific) as indicated in figures and legends.

2.3 | Western blotting

Transfected cells were scraped with hot lysis buffer (50 mM Tris pH 6.8, 2% SDS, 10% glycerol, 100 mM dithiothreitol), sonicated, boiled for 10 min, centrifuged at top speed at room temperature for 10 min, and loaded onto SDS-PAGE gels (4%–20% gradient gels, Bio-Rad). They were then transferred onto PVDF membrane and incubated with antibodies as indicated in figures. Western blots were developed using the charge-coupled device-equipped Syngene PXi 4 or Bio-Rad's ChemiDoc. Blots were quantified using ImageLab software (Bio-Rad). For loading controls, we conducted direct blue staining of PVDF membranes. Membranes were submerged for 5–10 min in 0.008% Direct Blue 71 (Sigma-Aldrich) in 40% ethanol and 10% acetic acid, rinsed briefly in 40% ethanol and 10% acetic acid solvent, followed by brief rinses in ultrapure water, air dried, and imaged and quantified similar to images from Western blotting. SDS-PAGE loading and Western blotting imaging was conducted by individuals different than the ones conducting transfections and collecting lysates, and sample identity was blinded before loading.

2.4 | qRT-PCR

Each qRT-PCR experiment was conducted using transfection samples collected on the same day from the same batch of cells, ensuring that comparisons were made among samples that had the same environment/cell culture conditions. Total RNA was extracted from transfected cells using TRIzol (Thermo Fisher). Extracted RNA was treated with TURBO DNA-free™ DNase (Ambion). Reverse transcription was carried out using High-Capacity cDNA Reverse Transcription Kit (Thermo Fisher). mRNA levels were quantified using Fast SYBR Green Master Mix (Thermo Fisher) with StepOne Real-Time PCR system. Primers used were as follows: MJD-F: 5'-GAATGGCAGAAGGAGGAGTTACTA-3'; MJD-R: 5'-GACCCGTCAAGAGAGAATTCAAGT-3'; GFP-F: 5'-CAACAGC CACAACGTCTATATCAT-3'; GFP-R: 5'-GGTGTTCTGCTGG TAGTGGTC-3'; GAPDH-F: 5'-CTCAGACACCATGGGGAAGGT-3'; GAPDH-R: 5'-GTGGTGCAGGAGGCATTGCTGA-3'.

2.5 | *In silico* analyses

The C-terminal sequence of isoform 2 of ataxin-3, highlighted in Figures 1 and 4, was input into the BLASTp website (https://blast.ncbi.nlm.nih.gov/Blast.cgi?PAGE=Proteins) with the following options selected: nonredundant protein sequences (nr) and no specific species indicated. For IUPred (https://iupred2a.elte.hu; (Meszaros, Erdos, & Dosztanyi, 2018)), FoldIndex (https://fold.weizmann.ac.il/fldbin/findex; Prilusky et al., 2005; van der Lee et al., 2014)) and PONDR (http://www.pondr.com; Obradovic et al., 2003; Peng et al., 2005)), the full-length amino acid sequences of non polyQ-expanded ataxin-3 (Figure 1) were input into each program.

2.6 | Statistical analyses

As noted in the figure legends, Mann–Whitney *U* (MWU) test, ANOVA or student's *t*-tests were conducted to assess differences among groups at a statistical level. Data points that were used for analyses came from independent biological repeats. Most statistical comparisons were made using the MWU test. For MG132 and chloroquine studies, the

p values provided are from one-tailed tests. One-tailed tests were chosen in these cases because we were testing the hypothesis that MG132 or chloroquine leads to an increase (a change in only one direction) in protein levels of ataxin-3 or eGFP. For qRT-PCR studies, we made no predictions about directionality of fold change; therefore, two-tailed significance was computed. Where noted, *p* values were determined using the student's *t*-test; we and others have used this test before and it is generally accepted in the field. MWU and ANOVA were conducted using IBM SPSS Statistics and student's *t*-tests were done in Microsoft Excel.

3 | RESULTS AND DISCUSSION

3.1 | Ataxin-3 constructs and their stability in cultured mammalian cells

Our prior work with isoforms 1 and 2 of ataxin-3 presented the possibility that the C-terminus of isoform 2 is a degron. This notion arose from data where in-frame fusion of the tail of isoform 2 to the end of isoform 1 led to markedly lower protein levels of the hybrid protein (Johnson et al., 2019). The proteasome was key in this process, whereas autophagy had minimal impact. The possibility that the hydrophobic tail of isoform 2 acts as a degron should not be a surprise, since degrons often consist of hydrophobic sequences that trigger quality control steps to rid the cell of a specific protein (Ella et al., 2019).

To empirically investigate the possibility of the tail of isoform 2 functioning as a degron, we embarked on the research described here. Our prior work with both isoforms of the SCA3 protein involved the polyQ-expanded, mutant form of ataxin-3; we did not investigate the ability of the C-terminus of isoform 2 to also lead to lower protein levels of wild-type, nondisease-causing ataxin-3. Additionally, we did not test before whether a truncated form of isoform 2, which results from a SNP, is also present at lower protein levels (Figure 1, orange font). Therefore, we generated new ataxin-3 constructs that contain the three versions of this protein shown in Figure 1: isoform 1, isoform 2, and the truncated isoform 2. Each of these constructs has an HA-epitope tag at the C-terminus. We and others have shown that a small epitope tag either in the front or the back of the ataxin-3 protein does not influence the varying degradation rates of its isoforms ([Harris et al., 2010; Johnson et al., 2019] and additional, unpublished observations from the Todi laboratory).

Transient expression of these forms of wild-type ataxin-3 in cultured, mammalian HEK-293T cells leads to noticeably lower protein levels of isoform 2 than isoform 1 (Figure 2a). The version of isoform 2 that comes to a more abrupt end due to a SNP is also at significantly lower protein levels than isoform 1, indicative that even a portion of the hydrophobic tail of isoform 2 is sufficient to reduce the levels of ataxin-3 protein.

With the addition of the proteasome inhibitor, MG132, isoform 2 protein levels are higher and resemble the levels of DMSO-treated cells expressing isoform 1. The presence of MG132 generally leads to higher ataxin-3 protein levels, indicating the importance of proteasome activity in the overall stability of ataxin-3 (Figure 2a–c,e). Comparing the effect of proteasome inhibition on isoforms 1 and 2, it is clear that this machinery has a more marked impact on the protein levels of isoform 2 and isoform 2 truncated than isoform 1 (Figure 2f, top). Inhibition of the other major branch of cellular protein disposal, autophagy,

by using chloroquine either does not significantly increase ataxin-3 protein levels (isoform 1, Figure 2b), or leads to a smaller increase than proteasomal inhibition (isoform 2 and truncated isoform 2; Figure 2c,e). Interestingly, treatment with chloroquine actually leads to lower levels of isoform 1 of ataxin-3 (Figure 2b). The reason behind this finding is unclear, but it could be due to changes in proteasome activity when autophagy is perturbed; we did not observe a similar reduction in ataxin-3 protein levels with chloroquine treatment with other variants of this protein (Figure 2). Based on these data, we conclude that the proteasome is the primary degradative machinery of ataxin-3, confirming our prior results in *Drosophila* and in cultured mammalian cells (Johnson et al., 2019).

Most proteins in eukaryotic cells require ubiquitination to be degraded by the proteasome (Varshavsky, 2017). We showed before that isoform 1 of ataxin-3 does not require its own ubiquitination to be turned over in mammalian cells or *in vivo*, in *Drosophila*: ubiquitinatable and nonubiquitinatable ataxin-3 isoform 1 species were at comparable protein levels and were degraded at comparable rates, according to pulse-chase experiments (Blount et al., 2014; Tsou et al., 2013). In fact, the nonubiquitinatable counterpart of isoform 1 might be degraded a little more rapidly (Blount et al., 2014; Tsou et al., 2013). We wondered whether the hydrophobic tail of isoform 2 requires ubiquitination to be degraded. We replaced each lysine residue in ataxin-3 with the similar, but nonubiquitinatable amino acid, arginine. These constructs are denoted here as “K-null”.

The “K-null” constructs are based on extensive earlier work in which we showed that lysine-to-arginine replacements lead to ataxin-3 protein that is not ubiquitinated *in vitro*, in mammalian cells, or *in vivo* in *Drosophila* (Blount et al., 2014; Todi et al., 2010; Tsou et al., 2013). Under all experimental conditions tested, lysine-less ataxin-3 remained nonubiquitinated, as reported by Western blots from reconstituted *in vitro* reactions, mammalian cell and whole fly lysis, and from stringent immunopurification protocols ([Blount et al., 2014; Todi et al., 2010; Tsou et al., 2013] and other, unpublished results from the Todi laboratory). Additionally, the lysine-to-arginine mutations do not abrogate the catalytic ability of ataxin-3, or its described cellular and *in vivo* functions, indicating that these replacements do not cause folding issues that render ataxin-3 unrecognizable or entirely nonfunctional (Blount et al., 2014; Todi et al., 2010; Tsou et al., 2013).

As shown in Figure 2, lysine-less ataxin-3 isoforms 1 and 2 do not accumulate in cells compared to their lysine-containing counterparts (Figure 2a,b). In fact, isoform 2 K-null protein levels are noticeably lower than isoform 2 with intact lysine residues (Figure 2a). Were ubiquitination of isoform 2 necessary for its degradation, we would have expected that the levels of its lysine-less version would be increased. Inhibiting the proteasome with MG132 leads to significantly higher levels of the K-null versions of isoforms 1 and 2 (Figure 2a,b,d), suggesting that the protein levels of each ataxin-3 variant that is missing all lysine residues are still dependent on this machinery. Isoform 2K-null is significantly more impacted by proteasome inhibition than isoform 1K-null (Figure 2f, bottom), similar to our observations with their lysine-containing counterparts (Figure 2f, top). Autophagy inhibition via chloroquine has no significant impact (Figure 2b,d), highlighting the proteasome as being primarily important for the stability of lysine-less ataxin-3.

To ensure that the protein levels we observed with the different isoforms of ataxin-3 are not a direct result of differences at the mRNA level, we conducted qRT-PCR analyses. As summarized in Figure 2g, the mRNA levels of the ataxin-3 constructs were either significantly higher (isoform 1K-null and isoform 2K-null) or not statistically significantly different (isoform 2 and isoform 2 truncated) compared to mRNA levels of isoform 1. Alongside the protein data summarized above with DMSO- and MG132-treated cells, these results indicate that lower protein levels of isoform 2 and truncated isoform 2 stem from reduced protein stability compared to isoform 1. Additional support for this conclusion comes from Figure 2f, which shows a more substantial impact from proteasome inhibition on isoform 2 than isoform 1. The qRT-PCR data also suggest that not only is lysine-less ataxin-3 not more stable than the ubiquitinatable version, but that it might actually be more prone to degradation, further confirming that this protein does not need to be modified by ubiquitin to be turned over. Lastly, just as with wild-type ataxin-3, the polyQ-expanded version (Q80) does not accumulate when all of its lysines are mutated into arginine (Figure 2h). As also shown before (Johnson et al., 2019), addition of the C-terminus of isoform 2 onto the end of isoform 1 leads to lower protein levels of the resulting protein, in a proteasome activity-dependent manner. Based on the collective data in Figure 2, we conclude that the C-terminus of isoform 2 of ataxin-3 leads to the proteasomal degradation of its host protein in a ubiquitination-independent manner, and that even a portion of that C-terminus, as in the case of the truncated isoform 2, can perturb the stability of ataxin-3.

While degrons are generally thought to function by signaling degradation through a ubiquitination step, proteins also exist where ubiquitination is not an absolute requirement. Examples of other proteins that espouse degrons but are degraded by the proteasome in a ubiquitination-independent manner include ornithine decarboxylase, Rpn4, and thymidylate synthase, as well as p21, p53, and α-synuclein (Ella et al., 2019; Erales & Coffino, 2014; Sanchez-Lanzas & Castano, 2014). Our prior and current data indicate that ataxin-3 belongs to the group of proteins that can be degraded without the necessity of its own ubiquitination (Blount et al., 2014; Sutton et al., 2017; Todi et al., 2010; Tsou et al., 2013). This is not to say that circumstances might not exist where ubiquitination of ataxin-3 could enhance its targeting to the proteasome and subsequent degradation. After all, there are reports of ubiquitin ligases that interact with ataxin-3, increasing its ubiquitination and its proteasomal turnover (Jana et al., 2005; Matsumoto et al., 2004; Sanchez-Lanzas & Castano, 2014; Scaglione et al., 2011; Wang, Li, & Ye, 2006). These include CHIP and Parkin, two other proteins linked to human diseases. We have shown before that ataxin-3 is, in fact, ubiquitinated in cells and *in vivo*, and that CHIP can handily perform this task *in vitro* (Scaglione et al., 2011; Todi et al., 2009, 2010; Tsou et al., 2013). However, our studies consistently found that ataxin-3 ubiquitination primarily enhances the deubiquitinase activities of ataxin-3 and upregulates its cellular functions, without enhancing its own degradation by the proteasome (Todi et al., 2009, 2010; Tsou et al., 2013). As is usually the case with biological systems, most likely ubiquitination of ataxin-3 regulates several properties, depending on the status of the cell, the type of cell or tissue, and ataxin-3 functional partners at the time. At this point, suffice it to say that the hydrophobic C-terminus of isoform 2 of ataxin-3 adds one more layer of regulation to the properties of this protein in the cellular environment.

In all of our assays in this study, as well as in prior work (Johnson et al., 2019), isoform 2 of ataxin-3 is less stable than isoform 1. As a result of the differences at their C-termini, the two isoforms may also have different interacting partners (Harris et al., 2010; Johnson et al., 2019; Weishäupl et al., 2019). The question arises why there might be an evolutionary need for the production of two isoforms with different partners and half-lives in cells, especially for a protein that, according to knockout mouse lines, appears unnecessary *in vivo* (Reina, Nabet, Young, & Pittman, 2012; Reina, Zhong, & Pittman, 2010; Schmitt et al., 2007; Switonski et al., 2011)? Different functions have been ascribed to ataxin-3 in mammalian cell culture and in *Drosophila*: ER-associated degradation, adaptation to various types of stress–including heat shock and DNA damage–and neuroprotection against misfolded proteins (Costa Mdo & Paulson, 2012; Matos et al., 2019; Tsou et al., 2013; Tsou, Hosking, et al., 2015; Tsou, Ouyang, et al., 2015; Warrick et al., 2005; Weishäupl et al., 2019; Winborn et al., 2008). Yet, knockout of *Atxn3* in mice failed to yield clear anomalies under normal conditions, or on the background of an expanded *HTT* allele that causes Huntington's disease (Costa Mdo & Paulson, 2012; Matos, de Macedo-Ribeiro, & Carvalho, 2011; Schmitt et al., 2007; Switonski et al., 2011; Zeng, Tallaksen-Greene, Wang, Albin, & Paulson, 2013). The overall notion in the field is that ataxin-3 has pleiotropic functions that are cell-state dependent; we should also state here that most of these studies were conducted with isoform 1, while isoform 2 has garnered comparatively little attention. Perhaps isoform 1 is important for a proportion of these activities, whereas isoform 2 performs other, or partly overlapping duties. The hydrophobic tail of isoform 2 might serve both as an additional interaction site for functional partners of ataxin-3 and a self-regulatory signal for a version of this protein that might need to be degraded more rapidly once its roles are completed. Isoform 2 could also function as a regulatory element for the levels or activities of isoform 1. Clearly, additional studies are required to unfold the intricacies of the functions of ataxin-3 isoforms.

While our work shows the C-termini of isoforms 1 and 2 regulating the stability of the ataxin-3 protein, additional modulatory elements may exist beyond the protein-coding sequence of the *ATXN3* gene. For example, 3'-UTRs play important regulatory roles for their host genes (Beilharz, See, & Boag, 2019; Kurosaki, Popp, & Maquat, 2019; Mayr, 2017, 2020). Here, we focused on the coding region of ataxin-3 to rule out interference from 3'-UTR and polyA tails, but we recognize that the 3'-UTRs might also exert control at the level of gene expression or mRNA stability.

3.2 | Addition of the hydrophobic tail of ataxin-3 leads to lower eGFP protein levels

To examine the degron-like properties of the hydrophobic tail of isoform 2 of ataxin-3, we excised it from its natural context and added it to an unrelated protein, eGFP (Figure 3a). For a peptide to have degron properties it should impact not only the levels of the original protein, it should also enhance the degradation of other, unrelated hosts (Ella et al., 2019; Erales & Coffino, 2014; Varshavsky, 2019).

Transfection of the same amount of eGFP or eGFP+Iso2 Tail into HEK-293T cells leads to significantly lower steady-state protein levels of the eGFP version with the hydrophobic tail fused to it (Figure 3b). We confirmed that this result was at least in part due to increased

degradation rates of eGFP+Iso2 Tail through a cycloheximide (CHX)-based assay. CHX inhibits the translation of new protein, enabling us to monitor the disappearance of already produced protein over a period of time. We transfected the cells with eGFP or eGFP+Iso2 Tail, and supplemented the cells with CHX 24 hr later. As shown in Figure 3c, eGFP+Iso2 Tail is degraded more rapidly than eGFP in mammalian cells. Thus, the hydrophobic C-terminus of ataxin-3 isoform 2 can impact the turnover of an unrelated protein.

Next, we confirmed that the proteasome was involved in the stability of eGFP+Iso2 Tail. As shown in Figure 3d, incubating cells with MG132 leads to a sizeable and statistically significant increase in the levels of eGFP fused to the hydrophobic tail of ataxin-3. Treatment with MG132 also leads to slightly higher levels of unmodified eGFP, but those values do not reach statistical significance (Figure 3d). We additionally tested the effect of chloroquine and found that autophagy inhibition by this chemical does not have a statistically significant impact on the levels of either version of eGFP (Figure 3e,f). These data indicate the proteasome as the main determinant of steady-state levels of eGFP+Iso2 Tail and suggest that the impact of the hydrophobic tail fused to eGFP is at least in part proteasome dependent.

Lastly, we examined whether the effect of the isoform 2 tail on eGFP levels is due to quicker protein degradation, or if it also has an mRNA levels component. We conducted this analysis since the steady-state levels of eGFP+Iso2 Tail are markedly lower than eGFP (Figure 3b), but the CHX-based turnover rate is not as dramatically different (Figure 3c). As shown in Figure 3g, the mRNA levels of eGFP+Iso2 Tail were significantly lower than eGFP. It appears that in the context of eGFP the hydrophobic tail impacts not only the proteasomal degradation of eGFP, but also its mRNA, perhaps by altering its stability. Thus, the hydrophobic C-terminus of ataxin-3 isoform 2 regulates eGFP protein levels in part at a post-transcriptional level. It is important to note that in the context of full-length ataxin-3, the hydrophobic tail did not significantly lower mRNA levels *in vivo* in transgenic fly lines (Johnson et al., 2019) or in mammalian cells (Figure 2). In fact, the mRNA levels of ataxin-3 isoform 2 K-null were markedly higher than those of isoform 1 (Figure 2g), while the protein levels were markedly lower for isoform 2K-null than isoform 1 (Figure 2a). Based on results from full-length ataxin-3 in *Drosophila* (Johnson et al., 2019) and in mammalian cells (Figure 2), ataxin-3's hydrophobic C-terminus consistently reduces host protein levels, but does not consistently or unidirectionally affect its mRNA levels. Our overall findings that the fusion of the hydrophobic tail of isoform 2 of ataxin-3 to eGFP reduces its steady-state levels in a proteasome-dependent manner, while concomitantly increasing protein turnover rates lead us to conclude that this sequence expedites host protein degradation and functions as a degron.

Because the tail of isoform 2 leads to lower levels of eGFP protein, we wondered whether a sequence similar to this hydrophobic C-terminus is present in other proteins, representing a more widely used type of degradative signal. We conducted BLASTp analyses without species restrictions; that is, we compared the sequence of the hydrophobic tail of isoform 2 of ataxin-3 to all species that have been sequenced. As shown in Figure 4, the only proteins that emerged from this analysis were ataxin-3 versions among different primates that have an *Atxn3* gene; no other proteins with sequence similarity appeared. These results indicate

that the hydrophobic tail of isoform 2 does not exist in species other than the ones in Figure 4, and that any function or identity imparted onto ataxin-3 by this precise sequence does not extend beyond primates. Still, since BLASTp analysis is based on amino acid identity, it does not exclude the possibility that other proteins may utilize different amino acid sequences that fold similarly to the hydrophobic tail of ataxin-3 to increase protein degradation.

A recent study identified a large group of C-terminal degrons for eukaryotic proteins and the ubiquitin conjugase and ligase complexes that target them for degradation by the proteasome (Koren et al., 2018). Based on the sequences identified by that work, it does not appear that the tail of isoform 2 of ataxin-3 belongs to these degron-ubiquitin conjugation/ligation complexes. The fact that lysine-to-arginine mutations for the entire ataxin-3 sequence did not lead to its accumulation in cells further suggests that the hydrophobic sequence of ataxin-3 signals degradation independently of ubiquitination.

The difference at the C-termini of the two isoforms of ataxin-3 has clear consequences on the stability of the protein in mammalian cells and *in vivo*. For an additional glimpse into this region of the SCA3 protein, we used three programs that predict disorder/ order tendencies. Degrons tend to reside in disordered regions of proteins (Fishbain et al., 2015; Guharoy, Bhowmick, Sallam, & Tompa, 2016; van der Lee et al., 2014), suggesting that the tail of isoform 2 might be more disordered than that of isoform 1. Thus, determining the relative order/disorder of these isoforms' C-termini may provide clues into the type of degron associated with isoform 2. As shown in Figure 5, each of the three programs that we used–IUPred (Dosztanyi, Csizmok, Tompa, & Simon, 2005; Meszaros et al., 2018), FoldIndex (Prilusky et al., 2005; van der Lee et al., 2014) and PONDR (Obradovic et al., 2003; Peng et al., 2005)–suggests that the tail of isoform 2 is in fact more ordered than that of isoform 1, contradicting our prediction. Likely, it is not simply the hydrophobicity or general order/disorder index that underlies the degron capacity of the C-terminus of isoform 2, but also a specific folding pattern that enables enhanced degradation through protein–protein interactions.

A degron-containing protein's interaction partners can influence its degradation rate; for example, ornithine decarboxylase normally functions as a homodimer, but, when it forms a heterodimer with antizyme 1, a C-terminal degron is exposed and ornithine decarboxylase is subjected to ubiquitin-independent proteasomal degradation (Li & Coffino, 1992, 1993; Liu et al., 2011). According to recent results from the Schmidt laboratory, the tails of ataxin-3 isoforms lead to differential protein–protein interactions (Weishäupl et al., 2019). The nature of these interactions, any involvement that they might have in ataxin-3 stability, and the role of folding differences between the two variants of ataxin-3 await additional investigations.

Future work is required to dissect the precise mechanistic details through which the hydrophobic tail of isoform 2 of ataxin-3 regulates the stability of its host protein. Such studies would be ideally conducted in differentiated cell lines–representing the multitude of tissues and cell types that express ataxin-3–and in intact model organisms to understand the functions of ataxin-3 isoforms in a more physiological setting. After all, ataxin-3 is ubiquitously expressed and likely has divergent functions in different tissues and under

various physiological conditions. The work that we conducted here in cultured mammalian cells has inherent limitations as a result of their immortalized status and the introduction of exogenous species. However, these studies serve as a launching pad toward future investigations of this disease-causing protein and, alongside our prior work in *Drosophila* (Johnson et al., 2019), demonstrate a key role for the C-terminus of ataxin-3 in its protein levels.

4 | CONCLUDING REMARKS

We examined the degron capability of the C-terminus of isoform 2 of ataxin-3. We showed that the tail of the less stable isoform of this disease-causing protein enhances the degradation of its host in a ubiquitination-independent manner and also destabilizes an unrelated protein. Our studies identify the hydrophobic C-terminus of ataxin-3 isoform 2 as a degron.

Funding information

National Ataxia Foundation; Wayne State University; National Institute of Neurological Disorders and Stroke

DATA AVAILABILITY STATEMENT

All data pertinent to this work are included in figures. Additional images can be found at https://drive.google.com/open?id=1e3O12LPNnYCZdD8umT9QYqCNrpRO0nUo

REFERENCES

Amm I, Sommer T, & Wolf DH (2014). Protein quality control and elimination of protein waste: The role of the ubiquitin-proteasome system. Biochimica et Biophysica Acta, 1843(1), 182–196. 10.1016/j.bbamcr.2013.06.031 [PubMed: 23850760]

Beilharz TH, See MM, & Boag PR (2019). 3'-UTRs and the control of protein expression in space and time. Advances in Experimental Medicine and Biology, 1203, 133–148. 10.1007/978 [PubMed: 31811633]

Blount JR, Tsou W-L, Ristic G, Burr AA, Ouyang M, Galante H, … Todi, S. V. (2014). Ubiquitin-binding site 2 of ataxin-3 prevents its proteasomal degradation by interacting with Rad23. Nature Communications, 5, 4638. 10.1038/ncomm

Budenholzer L, Cheng CL, Li Y, & Hochstrasser M (2017). Proteasome structure and assembly. Journal of Molecular Biology, 429(22), 3500–3524. 10.1016/j.jmb.2017.05.027 [PubMed: 28583440]

Chau V, Tobias JW, Bachmair A, Marriott D, Ecker DJ, Gonda DK, & Varshavsky A (1989). A multiubiquitin chain is confined to specific lysine in a targeted short-lived protein. Science, 243(4898), 1576–1583. 10.1126/science.2538923 [PubMed: 2538923]

Ciechanover A, & Stanhill A (2014). The complexity of recognition of ubiquitinated substrates by the 26S proteasome. Biochimica et Biophysica Acta, 1843(1), 86–96. 10.1016/j.bbamcr.2013.07.007 [PubMed: 23872423]

Collins GA, & Goldberg AL (2017). The logic of the 26S proteasome. Cell, 169(5), 792–806. 10.1016/j.cell.2017.04.023 [PubMed: 28525752]

Costa Mdo C, & Paulson HL (2012). Toward understanding Machado-Joseph disease. Progress in Neurobiology, 97(2), 239–257. 10.1016/j.pneurobio.2011.11.006 [PubMed: 22133674]

der Lee R, Buljan M, Lang B, Weatheritt RJ, Daughdrill GW, Dunker AK, … Babu MM (2014). Classification of intrinsically disordered regions and proteins. Chemical Reviews, 114(13), 6589–6631. 10.1021/cr400525m [PubMed: 24773235]

Dosztanyi Z, Csizmok V, Tompa P, & Simon I (2005). The pairwise energy content estimated from amino acid composition discriminates between folded and intrinsically unstructured proteins. Journal of Molecular Biology, 347(4), 827–839. 10.1016/j.jmb.2005.01.071 [PubMed: 15769473]

Ella H, Reiss Y, & Ravid T (2019). The hunt for degrons of the 26S proteasome. Biomolecules, 9(6), 230. 10.3390/biom9

Erales J, & Coffino P (2014). Ubiquitin-independent proteasomal degradation. Biochimica et Biophysica Acta, 1843(1), 216–221. 10.1016/j.bbamcr.2013.05.008 [PubMed: 23684952]

Finley D (2009). Recognition and processing of ubiquitin-protein conjugates by the proteasome. Annual Review of Biochemistry, 78, 477–513. 10.1146/annur ev.bioch em.78. 081507.101607

Fishbain S, Inobe T, Israeli E, Chavali S, Yu H, Kago G, … Matouschek A (2015). Sequence composition of disordered regions fine-tunes protein half-life. Nature Structural & Molecular Biology, 22(3), 214–221. 10.1038/nsmb.2958

Grice GL, & Nathan JA (2016). The recognition of ubiquitinated proteins by the proteasome. Cellular and Molecular Life Sciences, 73(18), 3497–3506. 10.1007/s00018-016-2255-5 [PubMed: 27137187]

Guharoy M, Bhowmick P, Sallam M, & Tompa P (2016). Tripartite degrons confer diversity and specificity on regulated protein degradation in the ubiquitin-proteasome system. Nature Communications, 7, 10239. 10.1038/ncommsl0239

Harris GM, Dodelzon K, Gong L, Gonzalez-Alegre P, & Paulson HL (2010). Splice isoforms of the polyglutamine disease protein ataxin-3 exhibit similar enzymatic yet different aggregation properties. PLoS One, 5(10), e13695. 10.1371/journal.pone.0013695 [PubMed: 21060878]

Heride C, Urbe S, & Clague MJ (2014). Ubiquitin code assembly and disassembly. Current Biology, 24(6), R215–R220. 10.1016/j.cub.2014.02.002 [PubMed: 24650902]

Jana NR, Dikshit P, Goswami A, Kotliarova S, Murata S, Tanaka K, & Nukina N (2005). Co-chaperone CHIP associates with expanded polyglutamine protein and promotes their degradation by proteasomes. Journal of Biological Chemistry, 280(12), 11635–11640. 10.1074/jbc.M412042200

Jariel-Encontre I, Bossis G, & Piechaczyk M (2008). Ubiquitin-independent degradation of proteins by the proteasome. Biochimica et Biophysica Acta, 1786(2), 153–177. 10.1016/j.bbcan.2008.05.004 [PubMed: 18558098]

Johnson SL, Blount JR, Libohova K, Ranxhi B, Paulson HL, Tsou WL, & Todi SV (2019). Differential toxicity of ataxin-3 isoforms in Drosophila models of Spinocerebellar Ataxia Type 3. Neurobiology of Diseases, 132, 104535. 10.1016/j.nbd.2019.104535

Koren I, Timms RT, Kula T, Xu Q, Li MZ, & Eiledge SJ (2018). The eukaryotic proteome is shaped by E3 ubiquitin ligases targeting C-terminal degrons. Cell, 173(7), 1622–1635.e1614. 10.1016/j.cell.2018.04.028 [PubMed: 29779948]

Kraut DA, Prakash S, & Matouschek A (2007). To degrade or release: Ubiquitin-chain remodeling. Trends in Cell Biology, 17(9), 419–421. 10.1016/j.tcb.2007.06.008 [PubMed: 17900906]

Kurosaki T, Popp MW, & Maquat LE (2019). Quality and quantity control of gene expression by nonsense-mediated mRNA decay. Nature Reviews Molecular Cell Biology, 20(7), 406–420. 10.1038/s41580-019-0126-2 [PubMed: 30992545]

Li X, & Coffino P (1992). Regulated degradation of ornithine decarboxylase requires interaction with the polyamine-inducible protein antizyme. Molecular and Cellular Biology, 12(8), 3556–3562. 10.1128/mcb.l2.8.3556 [PubMed: 1630460]

Li X, & Coffino P (1993). Degradation of ornithine decarboxylase: Exposure of the C-terminal target by a polyamine-inducible inhibitory protein. Molecular and Cellular Biology, 13(4), 2377–2383. 10.1128/mcb.13.4.2377 [PubMed: 8455617]

Liu YC, Hsu DH, Huang CL, Liu YL, Liu GY, & Hung HC (2011). Determinants of the differential antizyme-binding affinity of ornithine decarboxylase. PLoS One, 6(11), e26835. 10.1371/journal.pone.0026835 [PubMed: 22073206]

Lucas X, & Ciulli A (2017). Recognition of substrate degrons by E3 ubiquitin ligases and modulation by small-molecule mimicry strategies. Current Opinion in Structural Biology, 44, 101–110. 10.1016/j.sbi.2016.12.015 [PubMed: 28130986]

Matos CA, de Almeida LP, & Nobrega C (2019). Machado-Joseph disease/spinocerebellar ataxia type 3: Lessons from disease pathogenesis and clues into therapy. Journal of Neurochemistry, 148(1), 8–28. 10.llll/jnc.14541 [PubMed: 29959858]

Matos CA, de Macedo-Ribeiro S, & Carvalho AL (2011). Polygiutamine diseases: The special case of ataxin-3 and Machado-Joseph disease. Progress in Neurobiology, 95(1), 26–48. 10.1016/j.pneurobio.2011.06.007 [PubMed: 21740957]

Matsumoto M, Yada M, Hatakeyama S, Ishimoto H, Tanimura T, Tsuji S, … Nakayama KI (2004). Molecular clearance of ataxin-3 is regulated by a mammalian E4. EMBO Journal, 23(3), 659–669. 10.1038/sj.emboj.7600081

Mayr C (2017). Regulation by 3'-untranslated regions. Annual Review of Genetics, 51, 171–194. 10.1146/annurev-genet-120116-024704

Mayr C (2020). 3' UTRs regulate protein functions by providing a nurturing niche during protein synthesis. Cold Spring Harbor Symposia on Quantitative Biology, 039206, 10.1101/sqb.2019.84.039206

Meszaros B, Erdos G, & Dosztanyi Z (2018). IUPred2A: Context-dependent prediction of protein disorder as a function of redox state and protein binding. Nucleic Acids Research, 46(Wl), W329–W337. 10.1093/nar/gky384 [PubMed: 29860432]

Obradovic Z, Peng K, Vucetic S, Radivojac P, Brown CJ, & Dunker AK (2003). Predicting intrinsic disorder from amino acid sequence. Proteins, 53(Suppl. 6), 566–572. 10.1002/prot.10532 [PubMed: 14579347]

Paulson HL (2007). Dominantly inherited ataxias: Lessons learned from Machado-Joseph disease/spinocerebellar ataxia type 3. Seminars in Neurology, 27(2), 133–142. 10.1055/s-2007-971172 [PubMed: 17390258]

Paulson HL, Das SS, Crino PB, Perez MK, Patel SC, Gotsdiner D, … Pittman, R. N. (1997). Machado-Joseph disease gene product is a cytoplasmic protein widely expressed in brain. Annals of Neurology, 41(4), 453–462. 10.1002/ana.410410408 [PubMed: 9124802]

Peng K, Vucetic S, Radivojac P, Brown CJ, Dunker AK, & Obradovic Z (2005). Optimizing long intrinsic disorder predictors with protein evolutionary information. Journal of Bioinformatics and Computational Biology, 3(1), 35–60. 10.1142/s0219720005000886 [PubMed: 15751111]

Prilusky J, Felder CE, Zeev-Ben-Mordehai T, Rydberg EH, Man O, Beckmann JS, … Sussman JL (2005). Foldlndex: A simple tool to predict whether a given protein sequence is intrinsically unfolded. Bioinformatics, 21(16), 3435–3438. 10.1093/bioinformatics/bti537 [PubMed: 15955783]

Reina CP, Nabet BY, Young PD, & Pittman RN (2012). Basal and stress-induced Hsp70 are modulated by ataxin-3. Cell Stress and Chaperones, 17(6), 729–742. 10.1007/sl2192-012-0346-2 [PubMed: 22777893]

Reina CP, Zhong X, & Pittman RN (2010). Proteotoxic stress increases nuclear localization of ataxin-3. Human Molecular Genetics, 19(2), 235–249. 10.1093/hmg/ddp482 [PubMed: 19843543]

Ristic G, Sutton JR, Libohova K, & Todi SV (2018). Toxicity and aggregation of the polyglutamine disease protein, ataxin-3 is regulated by its binding to VCP/p97 in *Drosophila melanogaster*. Neurobiology of Diseases, 116, 78–92. 10.1016/j.nbd.2018.04.013

Ristic G, Tsou WL, & Todi SV (2014). An optimal ubiquitin-prote-asome pathway in the nervous system: The role of deubiquitinating enzymes. Frontiers in Molecular Neuroscience, 7, 72. 10.3389/fnmol.2014.00072 [PubMed: 25191222]

Saeki Y (2017). Ubiquitin recognition by the proteasome. Journal of Biochemistry, 161(2), 113–124. 10.1093/jb/mvw091 [PubMed: 28069863]

Sanchez-Lanzas R, & Castano JG (2014). Proteins directly interacting with mammalian 20S proteasomal subunits and ubiquitin-independent proteasomal degradation. Biomolecules, 4(4), 1140–1154. 10.3390/biom4041140 [PubMed: 25534281]

Scaglione KM, Zavodszky E, Todi SV, Patury S, Xu P, Rodríguez-Lebrón E, … Paulson HL (2011). Ube2w and ataxin-3 coordinately regulate the ubiquitin ligase CHIP. Molecular Cell, 43(4), 599–612. 10.1016/j.molcel.2011.05.036 [PubMed: 21855799]

Schmidt J, Mayer AK, Bakula D, Freude J, Weber JJ, Weiss A, … Schmidt T (2019). Vulnerability of frontal brain neurons for the toxicity of expanded ataxin-3. Human Molecular Genetics, 28(9), 1463–1473. 10.1093/hmg/ddy437 [PubMed: 30576445]

Schmidt T, Landwehrmeyer GB, Schmitt I, Trottier Y, Auburger G, Laccone F, … Riess O (1998). An isoform of ataxin-3 accumulates in the nucleus of neuronal cells in affected brain regions of SCA3 patients. Brain Pathology, 8(4), 669–679. 10.1111/j.l750-3639.1998.tb00193.x [PubMed: 9804376]

Schmitt I, Linden M, Khazneh H, Evert BO, Breuer P, Klockgether T, & Wuellner U (2007). Inactivation of the mouse Atxn3 (ataxin-3) gene increases protein ubiquitination. Biochemical and Biophysical Research Communications, 362(3), 734–739. 10.1016/j.bbrc.2007.08.062 [PubMed: 17764659]

Schreiber A, & Peter M (2014). Substrate recognition in selective autophagy and the ubiquitin-proteasome system. Biochimica et Biophysica Acta, 1843(1), 163–181. 10.1016/j.bbamcr.2013.03.019 [PubMed: 23545414]

Sutton JR, Blount JR, Libohova K, Tsou W-L, Joshi GS, Paulson HL, … Todi SV (2017). Interaction of the polyglutamine protein ataxin-3 with Rad23 regulates toxicity in Drosophila models of Spinocerebellar Ataxia Type 3. Human Molecular Genetics, 26(8), 1419–1431. 10.1093/hmg/ddx039 [PubMed: 28158474]

Switonski PM, Fiszer A, Kazmierska K, Kurpisz M, Krzyzosiak WJ, & Figiel M (2011). Mouse ataxin-3 functional knock-out model. NeuroMolecular Medicine, 13(1), 54–65. 10.1007/S12017-010-8137-3 [PubMed: 20945165]

Thibaudeau TA, & Smith DM (2019). A practical review of proteasome pharmacology. Pharmacological Reviews, 71(2), 170–197. 10.1124/pr.117.015370 [PubMed: 30867233]

Thrower JS, Hoffman L, Rechsteiner M, & Pickart CM (2000). Recognition of the polyubiquitin proteolytic signal. EMBO Journal, 19(1), 94–102. 10.1093/emboj/19.l.94

Todi SV, Scaglione KM, Blount JR, Basrur V, Conlon KP, Pastore A, … Paulson HL (2010). Activity and cellular functions of the deubiquitinating enzyme and polyglutamine disease protein ataxin-3 are regulated by ubiquitination at lysine 117. Journal of Biological Chemistry, 285(50), 39303–39313. 10.1074/jbc.M110.181610

Todi SV, Winborn BJ, Scaglione KM, Blount JR, Travis SM, & Paulson HL(2009). Ubiquitination directly enhances activity of the deubiquitinating enzyme ataxin-3. EMBO Journal, 28(4), 372–382. 10.1038/emboj.2008.289

Tsou WL, Burr AA, Ouyang M, Blount JR, Scaglione KM, &Todi, S. V. (2013). Ubiquitination regulates the neuroprotective function of the deubiquitinase ataxin-3 in vivo. Journal of Biological Chemistry, 288(48), 34460–34469. 10.1074/jbc.M113.513903

Tsou WL, Hosking RR, Burr AA, Sutton JR, Ouyang M, Du X, … Todi SV (2015). DnaJ-1 and karyopherin alpha3 suppress degeneration in a new Drosophila model of Spinocerebellar Ataxia Type 6. Human Molecular Genetics, 24(15), 4385–4396. 10.1093/hmg/ddvl74 [PubMed: 25954029]

Tsou WL, Ouyang M, Hosking RR, Sutton JR, Blount JR, Burr AA, & Todi SV (2015). The deubiquitinase ataxin-3 requires Rad23 and DnaJ-1 for its neuroprotective role in *Drosophila melanogaster*. Neurobiology of Diseases, 82, 12–21. 10.1016/j.nbd.2015.05.010

Varshavsky A (2017). The ubiquitin system, autophagy, and regulated protein degradation. Annual Review of Biochemistry, 86, 123–128. 10.1146/annurev-biochem-061516--044859

Varshavsky A (2019). N-degron and C-degron pathways of protein degradation. Proceedings of the National Academy of Sciences of the United States of America, 116(2), 358–366. 10.1073/pnas.1816596116 [PubMed: 30622213]

Wang Q, Li L, & Ye Y (2006). Regulation of retrotranslocation by p97-associated deubiquitinating enzyme ataxin-3. Journal of Cell Biology, 174(7), 963–971. 10.1083/jcb.200605100

Warrick JM, Morabito LM, Bilen J, Gordesky-Gold B, Faust LZ, Paulson HL, & Bonini NM (2005). Ataxin-3 suppresses polyglutamine neurodegeneration in Drosophila by a ubiquitin-associated mechanism. Molecular Cell, 18(1), 37–48. 10.1016/j.molcel.2005.02.030 [PubMed: 15808507]

Weishaupl D, Schneider J, Peixoto Pinheiro B, Ruess C, Dold SM, von Zweydorf F, … Schmidt T (2019). Physiological and pathophysiological characteristics of ataxin-3 isoforms. Journal of Biological Chemistry 294(2), 644–661. 10.1074/jbc.RA118.005801

Winborn BJ, Travis SM, Todi SV, Scaglione KM, Xu P, Williams AJ, … Paulson HL (2008). The deubiquitinating enzyme ataxin-3, a polyglutamine disease protein, edits Lys63 linkages in mixed linkage ubiquitin chains. Journal of Biological Chemistry, 283(39), 26436–26443. 10.1074/jbc.M803692200

Zeng L, Tallaksen-Greene SJ, Wang B, Albin RL, & Paulson HL (2013). The de-ubiquitinating enzyme ataxin-3 does not modulate disease progression in a knock-in mouse model of Huntington disease. Journal of Huntington's Disease, 2(2), 201–215. 10.3233/JHD-130058

Significance

A degron is an amino acid sequence that expedites the cellular turnover of its host protein. We investigated the degron capability of the hydrophobic C-terminus of isoform 2 of ataxin-3, a protein whose mutation causes spinocerebellar ataxia type 3. The C-terminus of isoform 2 of ataxin-3 destabilizes its host protein in a proteasome activity-dependent manner, but independently of the protein's ubiquitination status. Our findings confirm the C-terminus of ataxin-3 isoform 2 as a degron and provide new insight into the cellular handling of this disease protein.

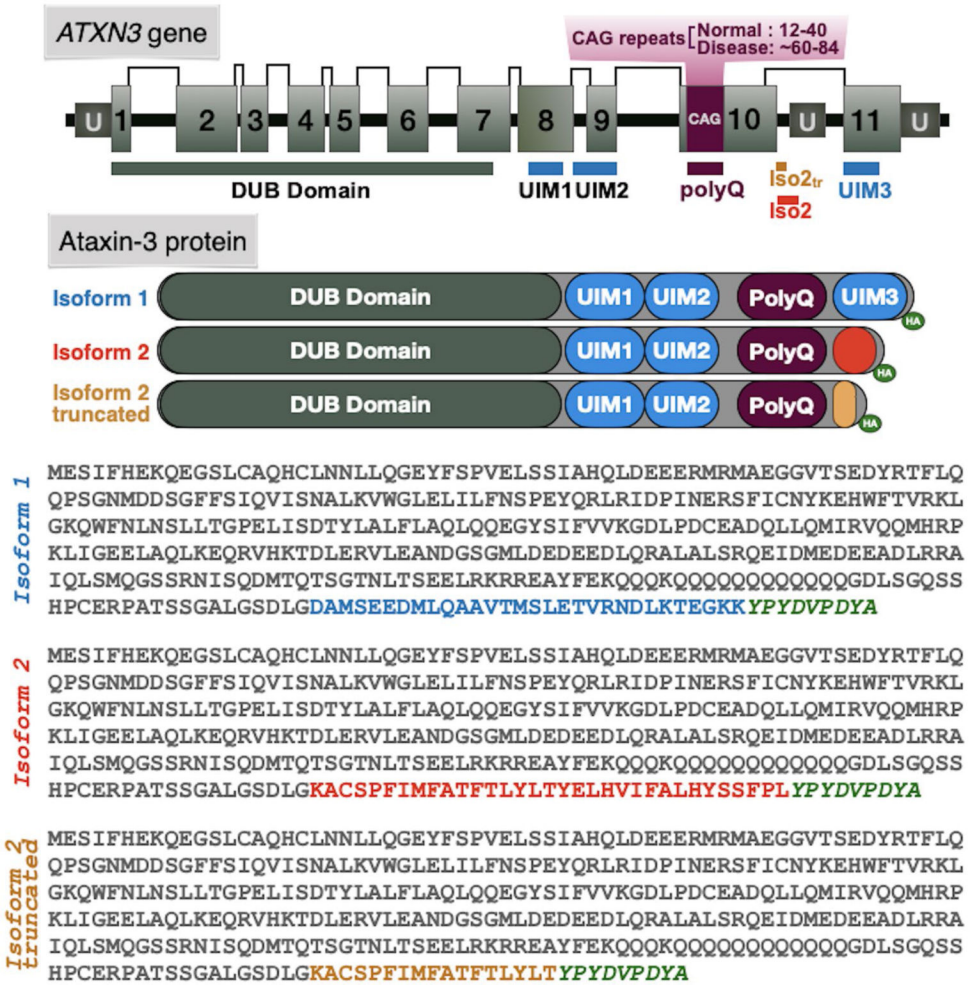

FIGURE 1.

Ataxin-3 isoforms. Diagrammatic representation of the human *ATXN3* gene and the ataxin-3 protein isoforms that arise from its differential splicing. $Iso2_{tr}$: a single-nucleotide polymorphism leads to a truncated version of isoform 2. DUB, deubiquitinase; PolyQ, polyglutamine; UIM, Ubiquitin-Interacting Motif; U, untranslated regions. Sequences below show the amino acid composition of the human ataxin-3 isoforms. Common regions are in gray lettering. The HA tag that is appended in frame at the C-terminal end is shown in green font

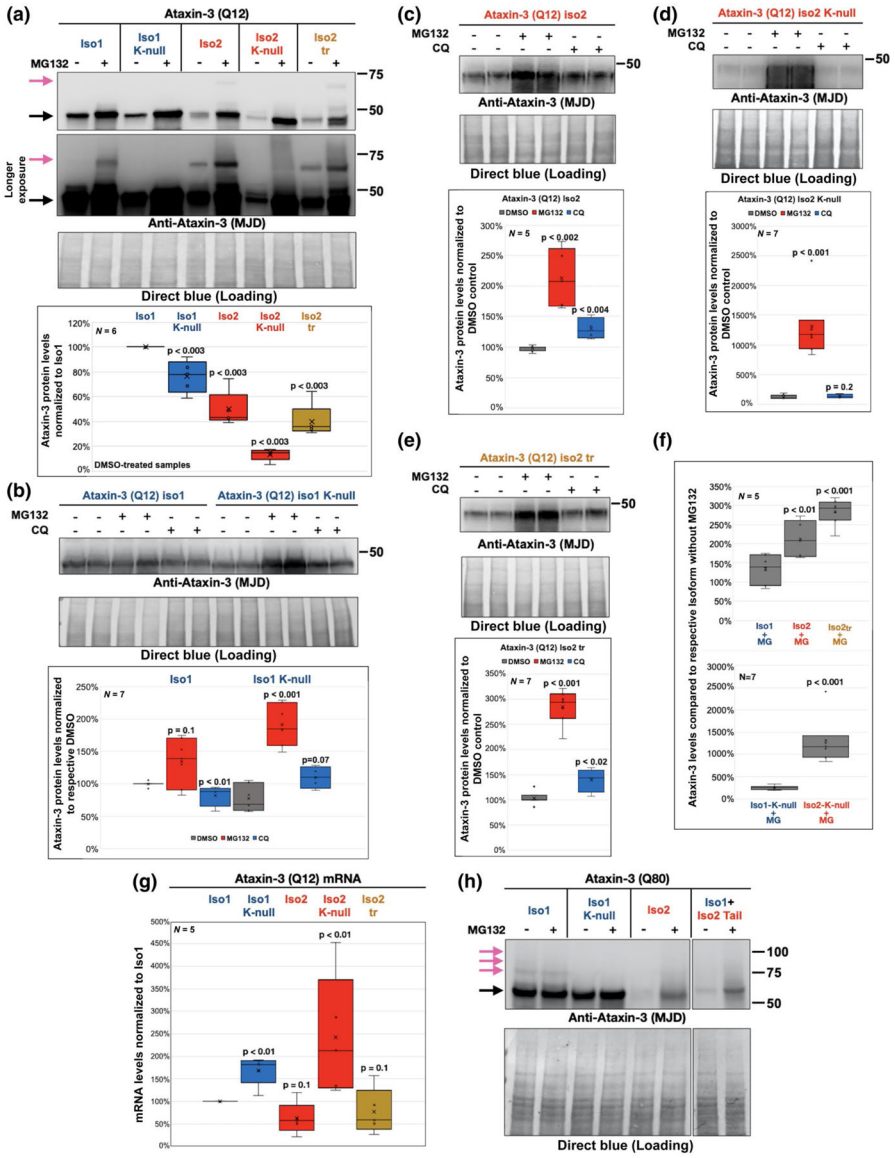

FIGURE 2.

Isoform 2 of ataxin-3 is present at lower protein levels in mammalian cells. (a–e) Western blots from whole cell lysates of HEK-293T cells transfected with ataxin-3 with a normal polyQ of 12 repeats, as indicated. Where noted, cells were treated overnight with DMSO, 20 μM MG132 (MG; in DMSO) or 100 μM chloroquine (CQ; in DMSO). Graphs in panels a–e are box-and-whisker plots of data quantified from respective images above each graph and other, independent biological replicates. *p* values for panels b–e are from one-tailed Mann-Whitney *U* tests comparing MG132- or chloroquine-treated cells to their DMSO-treated counterparts. *p* values for panel a are two-tailed Mann–Whitney *U* tests comparing all variants to “Iso1.” (f) Box-and-whisker plots comparing the effect of MG132 treatment on the isoforms of ataxin-3. Data were compiled by graphing values from MG132-treated, HEK-293T cells expressing the denoted isoforms, normalized to their respective, DMSO-treated cells and expressed as percent change. *p* values are from two-tailed student’s *t*-tests

comparing isoform 2 to isoform 1 from data in panels b–e and other, independent biological replicates. (g) qRT-PCR data measuring the noted mRNA levels compared statistically to isoform 1. *p* values are from two-tailed Mann–Whitney *U* tests. (h) Western blots from HEK-293T cells transfected with ataxin-3 constructs harboring an expanded polyQ of 80 repeats. Lanes are from the same blot and same exposure, cropped and rearranged for ease of viewing. In panels a and h: black arrows denote the main, unmodified band of ataxin-3 protein and purple arrows denote ubiquitinated species of ataxin-3 that we sometimes, but not always, observe in this type of assay. In all graphs, “N”s denote independent biological replicates

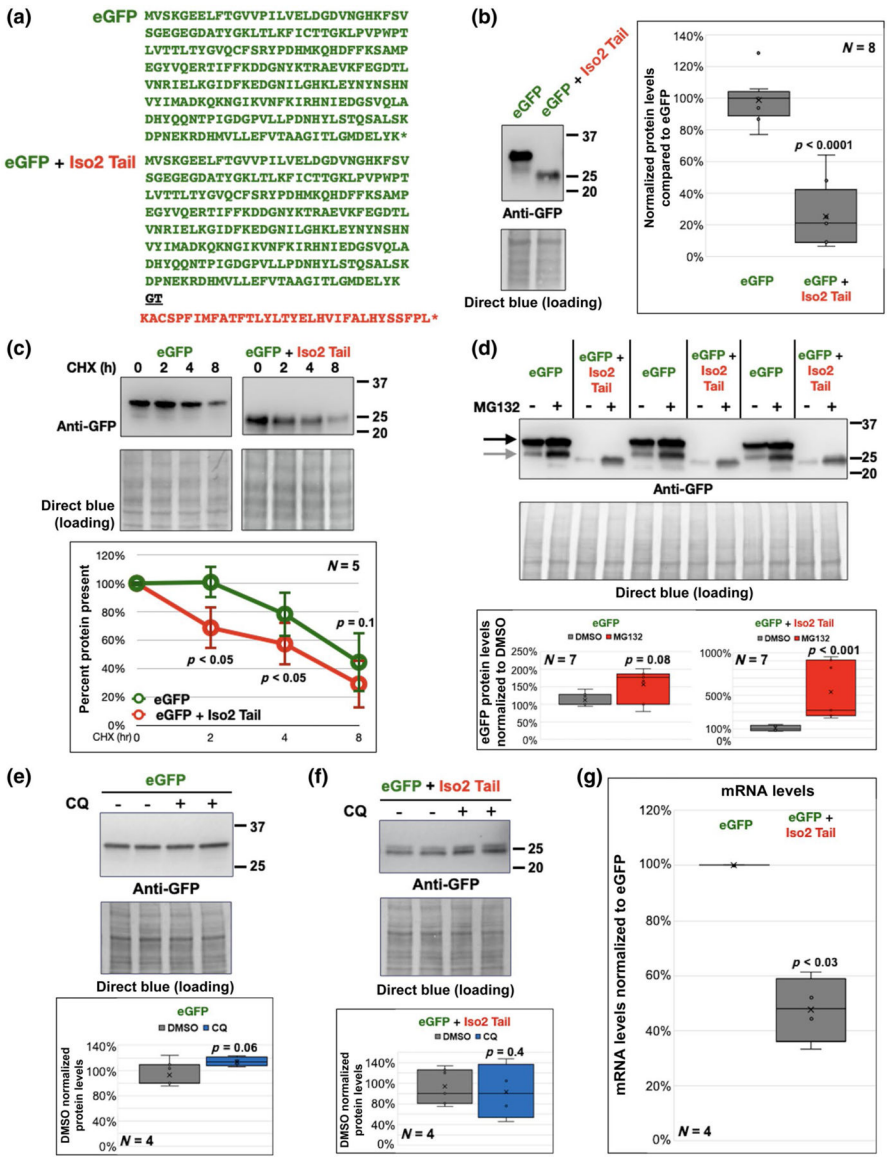

FIGURE 3.

The tail of isoform 2 of ataxin-3 reduces eGFP stability in mammalian cells. (a) Construct design. Underlined amino acids in black font result from cloning. (b) Steady-state levels of eGFP variants transfected into HEK-293T cells and harvested 24 hr later. Whole cell lysates. Graph is from images on the left and other, independent biological replicates. *p* value is from two-tailed Mann–Whitney *U* test. (c) Whole cell lysates of HEK-293T cells transfected as noted and treated with cycloheximide (CHX; 100 μM) 24 hr later for the indicated amounts of time. Images are from the same membrane, exposed for different amounts of time to approximate t=0 hr levels of the two constructs. Graph below is from quantification of signal from images above and other, independent biological repeats. *p* values are from student's *t*-tests comparing levels at each respective point for "eGFP+Iso2 Tail" to "eGFP." Similar results were obtained from ANOVA with Tukey's post hoc. (d–f) Steady-state levels of eGFP variants from whole cell lysates. HEK-293T cells were transfected as indicated and 24

hr later were treated overnight with MG132 (20 μM) or chloroquine (CQ; 100 μM) dissolved in DMSO, or with DMSO alone. Black arrow in panel d: main eGFP band. Gray arrow in panel d: another anti-GFP-positive band that we observe sometimes, but not always, that might be a proteolytic fragment of full eGFP. Graphs in panels d–f are from respective images on top and additional biological repeats. *p* values are from one-tailed Mann–Whitney *U* tests comparing MG132- or chloroquine-treated cells to DMSO-treated counterparts. For panels b–f: Note that "eGFP+Iso2 Tail" migrates more quickly on SDS-PAGE gels than "eGFP," similar to what we observed before with ataxin-3 isoform 2 in flies (Johnson et al., 2019) and in mammlian cells ((Johnson et al., 2019); Figure 2). This pattern most likely results from the hydrophobicity of the tail of isoform 2, which leads host proteins to migrate not quite as expected on SDS-PAGE gels. As with all other plasmids used in this work, plasmid identity and integrity was confirmed with site-restricted digests and two rounds of sequencing, which confirmed that "eGFP+Iso2 Tail" was intact. (g) qRT-PCR results comparing the levels of "eGFP" to "eGFP+Iso 2 Tail." *p* value is from two-tailed Mann–Whitney *U* test. "N"s in all graphs denote independent biological replicates

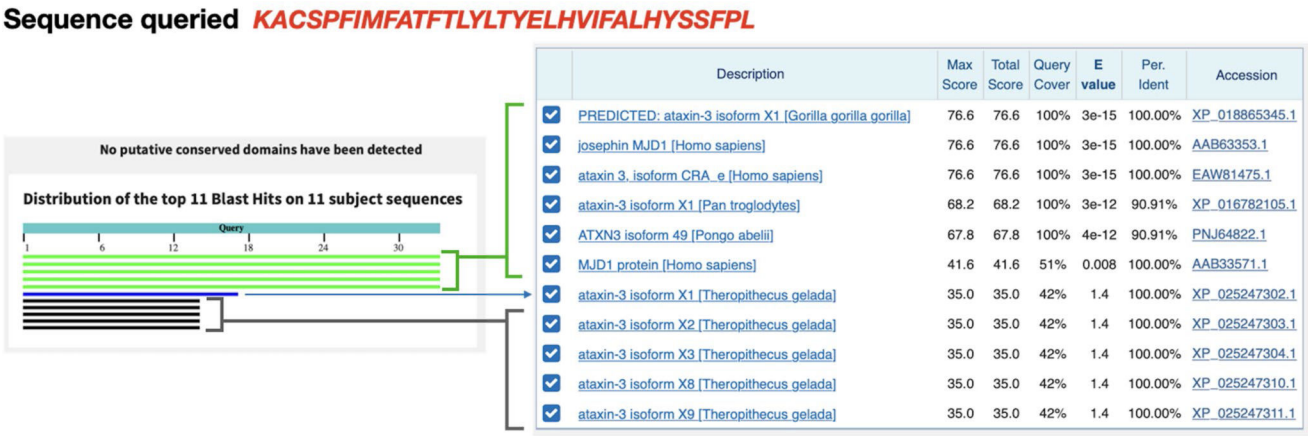

	Description	Max Score	Total Score	Query Cover	E value	Per. Ident	Accession
☑	PREDICTED: ataxin-3 isoform X1 [Gorilla gorilla gorilla]	76.6	76.6	100%	3e-15	100.00%	XP_018865345.1
☑	josephin MJD1 [Homo sapiens]	76.6	76.6	100%	3e-15	100.00%	AAB63353.1
☑	ataxin 3, isoform CRA_e [Homo sapiens]	76.6	76.6	100%	3e-15	100.00%	EAW81475.1
☑	ataxin-3 isoform X1 [Pan troglodytes]	68.2	68.2	100%	3e-12	90.91%	XP_016782105.1
☑	ATXN3 isoform 49 [Pongo abelii]	67.8	67.8	100%	4e-12	90.91%	PNJ64822.1
☑	MJD1 protein [Homo sapiens]	41.6	41.6	51%	0.008	100.00%	AAB33571.1
☑	ataxin-3 isoform X1 [Theropithecus gelada]	35.0	35.0	42%	1.4	100.00%	XP_025247302.1
☑	ataxin-3 isoform X2 [Theropithecus gelada]	35.0	35.0	42%	1.4	100.00%	XP_025247303.1
☑	ataxin-3 isoform X3 [Theropithecus gelada]	35.0	35.0	42%	1.4	100.00%	XP_025247304.1
☑	ataxin-3 isoform X8 [Theropithecus gelada]	35.0	35.0	42%	1.4	100.00%	XP_025247310.1
☑	ataxin-3 isoform X9 [Theropithecus gelada]	35.0	35.0	42%	1.4	100.00%	XP_025247311.1

FIGURE 4.

The tail of isoform 2 of ataxin-3 does not align with non-ataxin-3 proteins. Summary of findings from BLASTp analysis of the sequence shown in the figure. No specific organism was entered at the input stage. The amino acid sequence queried was blasted against all organisms. The species shown are the only ones that emerged from this analysis

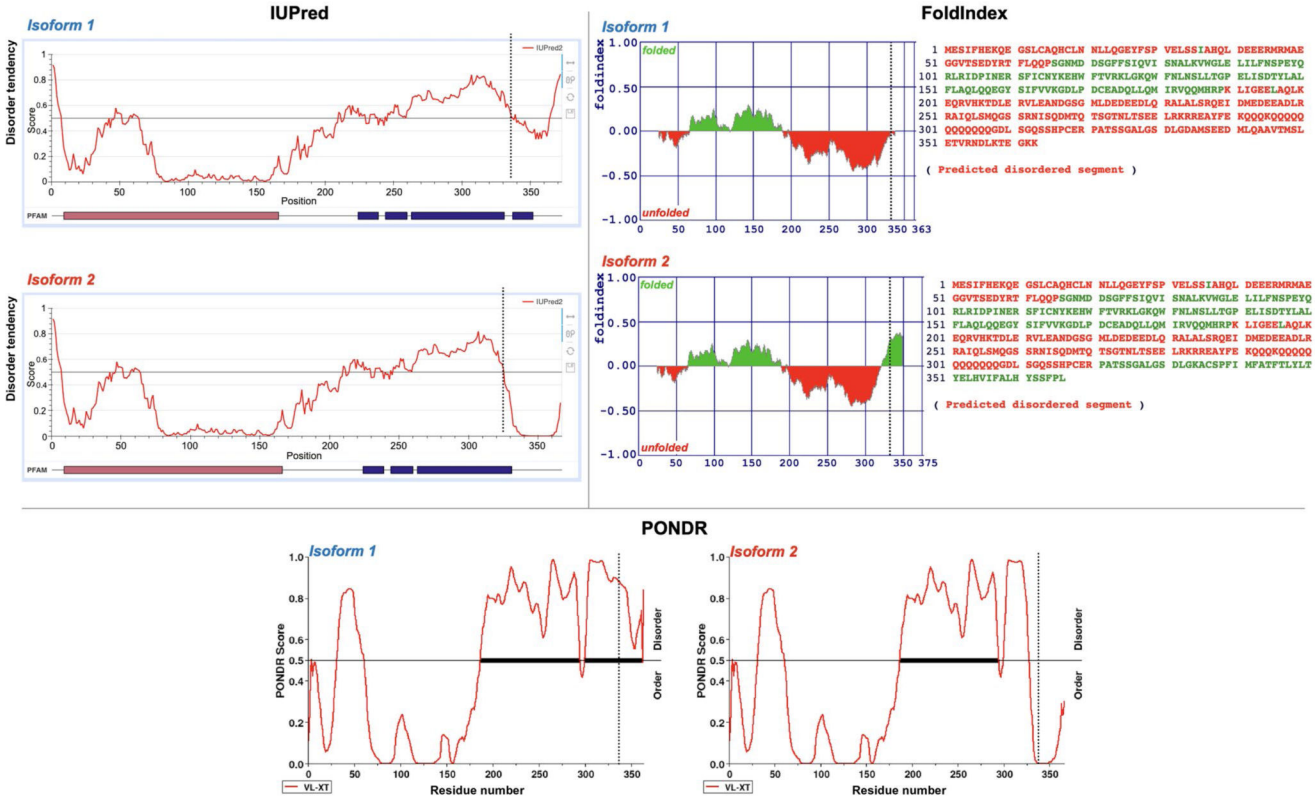

FIGURE 5.

Folding differences between isoforms 1 and 2 of ataxin-3. Shown are the results from three different folding prediction software programs (Materials and Methods) comparing the full-length sequences of isoforms 1 and 2 of wild-type ataxin-3. *Y*-axes indicate predicted order/disorder. Vertical dashed lines demarcate the tails of isoforms 1 and 2

TABLE 1

Summary of reagents and methods

Western blot						
Antibodies	Manufacturer	Concentration	Target antigen	Host	RRID	Figure
Primary anti-Ataxin-3 (MJD)	Gift from Dr. Henry Paulson	1:15,000	Full-length MJD/Ataxin-3 protein	Rabbit polyclonal	N/A	Figure 2
Primary anti-GFP	Cell Signaling Technology	1:1,000	GFP N-Terminus	Rabbit monoclonal	AB_ 1281300	Figure 3
Secondary anti-Rabbit	Jackson ImmunoResearch	1:10,000	Rabbit IgG (H+L)	Goat polyclonal	AB_ 2 3 07391	Figures 2 and 3
qRT-PCR						
Primers	Sequence					Figure
MJD-F	GAATGGCAGAAGGAGGAGTTACTA					Figure 2
MJD-R	GACCCGTCAAGAGAGAATTCAAGT					Figure 2
GFP-F	CAACAGCCACAACGTCTATATCAT					Figure 3
GFP-R	GGTGTTCTGCTGGTAGTGGTC					Figure 3
GAPDH-F	GCTCAGACACCATGGGGAAGGT					Figures 2 and 3
GAPDH-R	GTGGTGCAGGAGGCATTGCTGA					Figures 2 and 3
Software tools						
Names	Website				RRID	Figure
BLASTp	https://blast.ncbi.nlm.nih.gov/Blast.cgi?PAGE=Proteins				SCR _ 001010	Figure 4
UPred	https://iupred2a.elte.hu				N/A	Figure 5
FoldIndex	https://fold.weizmann.ac.il/fldbin/findex				N/A	Figure 5
PONDR	http://www.pondr.com				N/A	Figure 5